

# Detecting Human-Object Interactions via Functional Generalization

Ankan Bansal      Sai Saketh Rambhatla      Abhinav Shrivastava      Rama Chellappa  
University of Maryland, College Park  
{ankan, rssaketh, abhinav, rama}@umiacs.umd.edu

## Abstract

We present an approach for detecting human-object interactions (HOIs) in images, based on the idea that humans interact with functionally similar objects in a similar manner. The proposed model is simple and uses the visual features of the human, relative spatial orientation of the human and the object, and the knowledge that functionally similar objects take part in similar interactions with humans. We provide extensive experimental validation for our approach and demonstrate state-of-the-art results for HOI detection. On the HICO-Det dataset our method achieves a gain of over 7% absolute points in mean average precision (mAP) over published literature and even a gain of over 2.5% absolute mAP over contemporary work. We also show that our approach leads to significant performance gains for zero-shot HOI detection in the seen object setting. We further demonstrate that using a generic object detector, our model can generalize to interactions involving previously unseen objects.

## 1. Introduction

Human-object interaction (HOI) detection is the task of localizing and inferring relationships between a human and an object, e.g., “eating an apple” or “riding a bike.” Given an input image, the standard representation for HOIs [1, 2, 3, 4] is a triplet  $\langle \text{human}, \text{predicate}, \text{object} \rangle$ , where human and object are represented by bounding boxes, and predicate is the interaction between this (human, object) pair. At first glance, it seems that this problem is a composition of the atomic problems of object detection [5, 6, 7, 8] (independently localizing humans and objects) and classification [9, 4] (post-hoc classifying their interaction). These atomic recognition tasks are certainly the building blocks of a variety of approaches for HOI understanding [9, 4, 10]; and the progress in these atomic tasks directly translates to improvements in HOI understanding. However, the task of HOI understanding comes with its own unique set of challenges [1, 11, 3].

These challenges are due to the combinatorial explosion



Figure 1: Illustration of common properties of HOI Detection. (Top row) Datasets are not exhaustively labeled. (Bottom row) Humans interact in a similar fashion with functionally similar objects - both persons could be eating either a burger, a hot dog, a sandwich, or a pizza.

of the possible interactions with increasing number of objects and predicates. For example, in the commonly used HICO-Det dataset [3] with 80 unique object classes and 117 predicates, there are 9,360 possible relationships. This number increases to more than  $10^6$  for larger datasets like Visual Genome [12] and HCVRD [13], which have hundreds of object categories and thousands of predicates. This, combined with the long-tail distribution of HOI categories, makes it difficult to collect labeled training data for all HOI triplets. A common solution to this problem is to arbitrarily limit the set of HOI relationships and only collect labeled images for this limited subset. For example, the HICO-Det benchmark has only about 600 unique relationships.

Even though these datasets can be used for training fully-supervised models for recognizing a limited set of HOI triplets, they do not address the problem completely. For example, consider the images shown in Figure 1 (top row)

from the challenging HICO-Det dataset. The three pseudo-synonymous relationships:  $\langle \text{human}, \text{hold}, \text{bicycle} \rangle$ ,  $\langle \text{human}, \text{sit\_on}, \text{bicycle} \rangle$ , and  $\langle \text{human}, \text{straddle}, \text{bicycle} \rangle$  are all possible for both these images; but only a subset is labeled for each. We argue that this is not a quality control issue while collecting a dataset, but a problem associated with the huge space of possible HOI relationships. It is enormously challenging to exhaustively label even the 600 unique HOIs, let alone all possible interactions between humans and objects. An HOI detection model that relies entirely on labeled data will be unable to recognize the relationship triplets that are not present in the dataset, but are common in the real-world. For example, a naïve model trained on HICO-Det cannot recognize the  $\langle \text{human}, \text{push}, \text{car} \rangle$  triplet because this triplet does not exist in the training set. The ability to recognize previously unseen relationships (zero-shot recognition) is a highly desirable capability for a HOI detection system.

In this work, we address the challenges discussed above using a model that leverages the common-sense knowledge that humans have similar interactions with objects that are functionally similar. The proposed model has an inherent ability to do zero-shot detection. Consider the images in Figure 1 (second row) with  $\langle \text{human}, \text{eat}, ? \rangle$  triplet. The person in either image could be eating a burger, a sandwich, a hot dog, or a pizza. Inspired by this, our key contribution is incorporating this common-sense knowledge in a model for generalizing HOI detection to functionally similar objects. This model utilizes visual appearance of a human, their relative geometry with the object, and language priors [14] to capture which objects afford similar predicates [15]. Such a model is able to exploit the large amount of contextual information present in the language priors to generalize HOIs across functionally similar objects.

In order to train this module, we need a list of functionally similar objects and labeled examples for the relevant HOI triplets, neither of which are readily available. To overcome this, we propose a way to train this model by: 1) using a large vocabulary of objects, 2) discovering functionally similar objects automatically, and 3) proposing data-augmentation, emulating the examples shown in Figure 1 (second row). To discover functionally similar objects in an unsupervised way, we use a combination of visual appearance features [16] and semantic word embeddings [14] to represent the objects in a “world set” (Open Images Dataset (OID) [17] in this paper). Note that the proposed method is not contingent on the world set. Any large dataset, like ImageNet [18], could replace OID. Finally, to emulate the examples shown in Figure 1 (second row), we use the human and object bounding boxes from a labeled interaction, the visual features from the human bounding box, and semantic word embeddings of all functionally similar objects. Notice that this step does not utilize the visual features for

objects, just their relative locations with respect to a human, enabling us to perform this data-augmentation.

The proposed approach achieves over 7% absolute improvement in mAP over the best published method for HICO-Det. Further, using a generic object detector, and the proposed functional generalization model lends itself directly to the zero-shot HOI triplet detection problem. We clarify that zero-shot detection is the problem of detecting HOI triplets for which the model has never seen any images. Knowledge about functionally similar objects enables our system to detect interactions involving objects not contained in the original training set. Using just this generic object detector, our model achieves state-of-the-art performance for HOI detection on the popular HICO-Det dataset in the zero-shot setting, improving over existing methods by several percentage points. Additionally, we show that the proposed approach can be used as a way to deal with social/systematic biases present in image captioning and other vision+language datasets [19, 20].

In summary, the contributions of this paper are: (1) a functional generalization model for capturing functional similarities between objects; (2) a method for training the proposed model; and (3) state-of-the-art results on HICO-Det in both fully-supervised and zero-shot settings.

## 2. Related Work

**Human-Object Interaction.** Early methods [21, 22, 23] relied on structured visual features which capture contextual relationships between humans and objects. Similarly, [10] used structured representations and spatial co-occurrences of body parts and objects to train models for HOI recognition. Gupta *et al.* [24, 25] adopted a Bayesian approach that integrated object classification and localization, action understanding, and perception of object reaction. Desai *et al.* [26] constructed a compositional model which combined skeleton models, poselets, and visual phrases.

More recently, with the release of large datasets [27, 12, 13, 2, 3], the problem of detecting and recognizing HOIs has attracted significant attention. This has been driven by HICO [27] which is a benchmark dataset for recognizing human-object interactions. The HICO-Det dataset [3] extended HICO by adding bounding box annotations. V-COCO [2] is a much smaller dataset containing 26 classes and about 10,000 images. On the other hand, HCVRD [13] and Visual Genome [12] provide annotations for thousands of relationship categories and hundreds of objects. However, they suffer from noisy labels. Therefore, we use the HICO-Det dataset to evaluate our approach in this paper.

Gkioxari *et al.* [4] designed a system which trains object and relationship detectors simultaneously on the same dataset and classifies a human-object pair into a fixed set of pre-defined relationship classes. This precludes the method from being useful for detecting novel relationships. Sim-

ilarly, [28] used pose and gaze information for HOI detection. Kolesnikov *et al.* [29] introduced the Box Attention module to a standard R-CNN and trained simultaneously for object detection and relationship triplet prediction. Graph Parsing Neural Networks [30] incorporated structural knowledge and inferred a parse graph in a message passing inference framework. In contrast, our method does not need iterative processing and requires only a single pass through a neural network.

Unlike most prior work, we do not directly classify into a fixed set of relationship triplets but into predicates. This helps us detect completely unseen interactions. The method which is the closest in spirit to our approach is [9] where the authors used a two branch structure with the first branch being responsible for detecting humans and predicting the predicates, and the second branch for detecting objects. Unlike our proposed approach, their method does not even consider the object while predicting the predicate. It solely depends on the appearance of the human. Also, they do not use any prior information from language. Our model utilizes implicit human appearance, the object label, human-object geometric relationship, and knowledge about similarities between objects. Hence, our model achieves much better performance than [9] using the combination of these factors.

We also distinguish our work from prior work [31, 32, 33, 34] on HOI recognition where the task is to recognize the interaction in an image but not to locate the actors and objects. We tackle the more difficult problem of detecting HOIs in this paper. However, similar to some work on HOI recognition, we also work with the idea of using language encoded by word vectors to train our generalization module.

**Zero-shot Learning.** Our work also ties well with recent work on zero-shot classification [35, 36, 37, 38] and the nascent field of zero-shot object detection (ZSD) [39, 40, 41]. Bansal *et al.* [39] proposed projecting images into the word-vector space to exploit the semantic properties of such spaces. They also discussed challenges associated with training and evaluating ZSD. A similar idea was used in [37] for zero-shot classification. Rahman *et al.* [41], on the other hand, used meta-classes to cluster semantically similar classes while keeping distinct classes separate. In this work, we also use word-vectors as additional semantic information to our generalization module. This, along with our approach for incorporating generalization during training, helps the model detect previously unseen HOIs.

### 3. Approach

Figure 2 represents our approach. The main novelty and contribution of the proposed approach lies in incorporating generalization through a language component. This is done by using functionally similar objects to train the model. During inference, we first detect humans and objects in the

image using our object detectors, which also give the corresponding (RoI-pooled [7]) feature representations. Each detected human-object pair is used to extract visual and language features which are used to estimate the predicate associated with the interaction. We describe each component of the model in detail and the training procedure in the following sections.

#### 3.1. Object Detection

For our experiment in the fully-supervised setting, we use an object detector fine-tuned on the HICO-Det dataset. For zero-shot detection and further experiments, we use a Faster-RCNN [42] based detector trained on the Open Images dataset (OID) [17]. This network can detect 545 object categories and we use it to obtain proposals for humans and objects in an image. The object detectors also output the ROI-pooled [7] features corresponding to these detections. All human-object pairs thus obtained are passed to our model which outputs probabilities for each predicate.

#### 3.2. Functional Generalization Module

Humans look similar when they are interacting with objects that are functionally similar. Leveraging this fact, the functional generalization module exploits object similarity encoded in word vectors, the relative spatial location of human and object boxes, and the implicit human appearance to estimate the predicate. At its core, it comprises an MLP, which takes as input the human and object word embeddings,  $w_h$  and  $w_o$ , the geometric relationship between the human and object boxes  $f_g$ , and the human visual feature  $f_h$ . The human embedding,  $w_h$ , helps in distinguishing between different words for humans (man/woman/boy/girl/person). The geometric feature is useful as the relative positions of a human and an object can help eliminate certain predicates. The human feature  $f_h$  is used as a representation for the appearance of the human. This appearance representation is added because the aim is to incorporate the idea that humans look similar while interacting with similar objects. For example, a person drinking from a cup looks similar while drinking from a glass or a bottle. The four features  $w_h$ ,  $w_o$ ,  $f_g$ , and  $f_h$  are concatenated and passed through the 2-layer MLP which predicts the probabilities for each predicate. All the predicates are considered independent. We now give details of different components in this model.

##### 3.2.1 Word embeddings

We use 300-D vectors from word2vec [14] to get the human and object embeddings  $w_h$  and  $w_o$ . These encode semantic knowledge and allow the model to discover previously unseen interactions between a human and objects by exploiting the semantic similarities between objects.

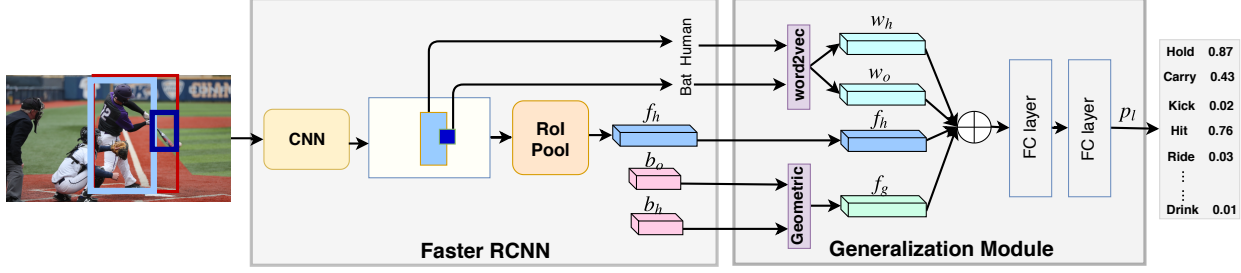


Figure 2: We detect all objects and humans in an image. This detector gives human features  $f_h$ , and the corresponding labels. We consider all pairs of human-object and create union boxes. Our functional generalization module uses the word vectors for the human  $w_h$ , the object class  $w_o$ , geometric features  $f_g$ , and  $f_h$  to produce the probability estimate over the predicates.

### 3.2.2 Geometric features

Following prior work on visual relationship detection [43], we define the geometric relationship feature as:

$$f_g = \left[ \frac{x_1^h}{W}, \frac{y_1^h}{H}, \frac{x_2^h}{W}, \frac{y_2^h}{H}, \frac{A^h}{A^I}, \frac{x_1^o}{W}, \frac{y_1^o}{H}, \frac{x_2^o}{W}, \frac{y_2^o}{H}, \frac{A^o}{A^I}, \right. \\ \left. \left( \frac{x_1^h - x_1^o}{x_2^o - x_1^o} \right), \left( \frac{y_1^h - y_1^o}{y_2^o - y_1^o} \right), \right. \\ \left. \log \left( \frac{x_2^h - x_1^h}{x_2^o - x_1^o} \right), \log \left( \frac{y_2^h - y_1^h}{y_2^o - y_1^o} \right) \right] \quad (1)$$

where,  $W, H$  are the image width and height,  $(x_i^h, y_i^h)$ , and  $(x_i^o, y_i^o)$  are the human and object bounding box coordinates respectively,  $A^h$  is the area of the human box,  $A^o$  is the area of the object box, and  $A^I$  is the area of the image. The geometric feature  $f_g$  uses spatial features for both entities (human and object) and also spatial features from their relationship. It is a measure of the scales and relative positioning of the two entities.

### 3.2.3 Generalizing to new HOIs

We incorporate the idea that humans interacting with similar objects look similar through the functional generalization module. As shown in figure 3, this idea can be added by changing the object name while keeping the human word vector  $w_h$ , the human visual feature  $f_h$ , and the geometric feature  $f_g$  fixed. Each object has a different word-vector and the model learns to recognize the same predicate for different human-object pairs. Note that this does not need visual examples for all human-object pairs.

**Finding similar objects.** An obvious choice for defining similarity between objects would be to find the closest objects in the WordNet hierarchy [44]. However, this creates several issues which make using WordNet impractical/ineffective. The first is defining distance between the nodes in the tree. The height of a node cannot be used as a metric because different things have different levels of

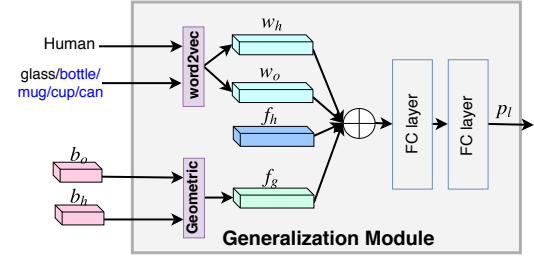


Figure 3: Generalization module. We can replace “glass” by “bottle”, “mug”, “cup”, or “can”.

categorization in the tree. Similarly, defining sibling relationships which adhere to functional intuitions is challenging. Another major issue with using WordNet is the lack of correspondence between closeness in the tree and semantic similarities between objects.

To overcome these problems, we consider similarity in both the visual and semantic representations of objects. We start by defining a vocabulary of objects  $\mathcal{V} = \{o_1, \dots, o_n\}$  which includes all the objects that can be detected by our object detector. For each object  $o_i \in \mathcal{V}$ , we obtain a visual feature  $f_{o_i} \in \mathbb{R}^p$  from images in OID, and a word vector  $w_{o_i} \in \mathbb{R}^q$ . We concatenate these two to obtain the mixed representation  $u_{o_i}$  for object  $o_i$ . We then cluster  $u_i$ 's into  $K$  clusters using Euclidean distance. Objects in the same cluster are considered functionally similar. This clustering has to be done only once. We use these clusters to find all objects similar to an object in the target dataset. Note that there might not be any visual examples for many of the objects obtained using this method. This is why we do not use the RoI-pooled visual features from the object.

We would like to point out that using either just the word2vec representations or just the visual representations for clustering gave several inconsistent clusters. Therefore, we use the concatenated features  $u_{o_i}$ . We observed that the clusters created using these features better correspond to functional similarities between objects.

**Generating training data.** For each relationship triplet  $\langle h, p, o \rangle$  in the original dataset, we add  $r$  triplets  $\langle h, p, o_1 \rangle$ ,



$\langle h, p, o_2 \rangle, \dots, \langle h, p, o_r \rangle$  to the dataset keeping the human, and object boxes fixed, and only changing the object name. This means that, for all these  $f_g$  and  $f_h$  are the same as for the original sample. The  $r$  different objects,  $o_1, \dots, o_r$  belong to the same cluster as object  $o$ . For example, in figure 3, the ground truth category “glass” can be replaced by “bottle”, “mug”, “cup”, or “can” while keeping  $w_h$ ,  $f_h$ , and  $f_g$  fixed.

### 3.3. Training

A training batch consists of  $T$  interaction triplets. The model produces the probabilities for each predicate independently. We use a weighted class-wise binary cross entropy loss for training the model.

We now describe a weighing strategy that can reduce the effects of lack of exhaustive labeling.

**Noisy labeling.** Missing and incorrect labels are a common issue in HOI datasets. Also, a human-object pair can have different types of interactions at the same time. For example, a person can be sitting on a bicycle, riding a bicycle, and straddling a bicycle. These interactions are usually labeled with slightly different bounding boxes. To overcome these issues, we use a per-triplet loss weighing strategy. A training triplet in our dataset has a single label, e.g.  $\langle \text{human-ride-bicycle} \rangle$ . A triplet with slightly shifted bounding boxes might have another label, like  $\langle \text{human-sit-on-bicycle} \rangle$ . The idea is that the models should be penalized more if they fail to predict the correct class for a triplet. Given the training sample  $\langle \text{human-ride-bicycle} \rangle$ , we want the model to definitely predict “ride”, but we should not penalize it if it predicts “sit\_on” as well. Therefore, while training the model, we use the following weighing scheme for classes. Suppose that a training triplet is labeled  $\langle \text{human-ride-bicycle} \rangle$  and there are other triplets in the image. For the training triplet under consideration, we assign a high weight to the loss for the correct class (ride), and a zero weight to all other predicates in the image. We also scale down the weight to the loss for all other classes to ensure that the model is not penalized too much for predicting a missing but correct label.

The final step of inference is class-wise non-maximal suppression (NMS) over the union bounding boxes (union of human and object boxes). This helps in removing multiple detections for the same interaction and leads to higher precision at the same recall.

## 4. Experiments

We evaluate our approach on the large-scale HICO-Det dataset [27].

### 4.1. Dataset and Evaluation Metrics

HICO-Det extends the HICO (Humans Interacting with Common Objects) dataset [27] which contains 600 HOI cat-

egories for 80 objects. HICO-Det gives bounding box annotations for humans, and objects for each HOI category. The training set of HICO-Det contains over 38,000 images and about 120,000 HOI annotations for 600 HOI classes. The test set has 9,600 images and 33,400 HOI instances.

For evaluation, HICO-Det uses the mean average precision (mAP) metric commonly used in object detection [45, 46]. Here, a HOI detection is counted as a true positive if the minimum of the human overlap  $\text{IOU}_h$  and object overlap  $\text{IOU}_o$  with the ground truth is greater than 0.5. Performance is usually reported for three different HOI category sets: (a) all 600 HOI categories (Full), (b) 138 categories with less than 10 training samples (Rare), and (c) the remaining 462 categories with more than 10 training samples (Non-Rare).

### 4.2. Implementation Details

We start with a Faster-RCNN-based object detector which is fine-tuned for the HICO-Det dataset. The base network for this detector is a ResNet-101. This detector was originally trained on the COCO dataset [46] which has the same 80 object categories as the HICO-Det dataset. We consider all detections for which the detection confidence is greater than 0.9 and create human-object pairs for each image. Each detection has an associated feature vector. These pairs are then passed through our model. The human feature  $f_h$  is 2048 dimensional. The two hidden layers in the model are of dimensions 1024 and 512. The model outputs probability estimates for each predicate independently and the final output prediction is all predicates with probability  $\geq 0.5$ .

For all the experiments, we train the complete model for 25 epochs with an initial learning rate of 0.1 which is dropped by one-tenth every 10 epochs. We re-iterate that the object detector and the word2vec vectors are frozen while training this model. For all experiments we use up to five ( $r$ ) additional objects for data augmentation. That is, for each human-object pair in the training set, we add up to five objects from the same cluster while leaving the bounding boxes and human features unchanged. We also describe zero-shot experiments where we show that our method can be used to detect previously unseen interactions.

### 4.3. Results

The last row in table 1 show the results obtained by our model. We observe that our model comprehensively outperforms all existing methods. It achieves an mAP of 21.96%, an almost 7% absolute improvement over the best published method [47] and even over 2.5% over the best contemporary work [48]. Also note the performance for rare classes. Our model achieves 16.43% mAP for rare classes compared to the existing best of 15.40%. The performance, along with the simplicity, of our model is a remarkable strength and

Table 1: mAPs (%) in the default setting for the HICO-Det dataset. Our model was trained with up to five neighbors for each object. The last column is the total number of parameters in the models where the first term is the number of parameters in the proposed classification model and the second term is the number of parameters in the object detector.

Method	Full (600 classes)	Rare (138 classes)	Non-rare (462 classes)	# Params (millions)
Shen <i>et al.</i> [9]	6.46	4.24	7.12	-
HO-RCNN + IP [3]	7.30	4.68	8.08	-
HO-RCNN + IP + S [3]	7.81	5.37	8.54	-
InteractNet [4]	9.94	7.16	10.77	-
iHOI [28]	9.97	7.11	10.83	-
GPNN [30]	13.11	9.34	14.23	-
ICAN [47]	14.84	10.45	16.15	48.1 + 40.9 = 89.0
Gupta <i>et al.</i> [49]	17.18	12.17	18.68	9.2 + 63.7 = 72.9
Interactiveness Prior [50]	17.22	13.51	18.32	35.0 + 29.0 = 64.0
Peyre <i>et al.</i> [51]	19.40	15.40	20.75	21.8 + 40.9 = 62.7
Ours	<b>21.96</b>	<b>16.43</b>	<b>23.62</b>	3.1 + 48.0 = 51.1

reveals that existing methods may be over-engineered.

#### Comparison of number of parameters

In table 1, we also compare the number of parameters in the four closest existing models against our model. With far fewer parameters, our model achieves better performance. For example, compared to the current state-of-the-art model which contains 62.7 million parameters and achieves only 19.40% mAP, our model contains just 51.1 million parameters and reaches an mAP of 21.96%. Ignoring the object detectors, our model introduces just 3.1 million new parameters. (Due to lack of specific details in previous papers, we have made some assumptions which we list in the supplementary materials. Wherever necessary, we have made conservative estimates for the number of parameters for prior methods.) Also, note that [49] and [50] also include a pose estimation model. The number of parameters in table 1 do not include pose estimation models. Our method provides a simple and intuitive way of thinking about the problem.

Next, we show how a generic object detector can be used to detect novel interactions, even those involving objects not present in the training set. For this, we use an off-the-shelf Faster RCNN-based object detector which is trained on the OpenImages dataset and is capable of detecting 545 object categories. This detector uses an Inception ResNet-v2 with atrous convolutions as its base network.

#### 4.4. Zero-shot HOI Detection

Recent work on zero-shot learning aims to either recognize [35] or detect [39] previously unseen objects in images. Shen *et al.* [9] take this idea further and try to detect previously unseen human-object relationships in images. This means that the aim is to detect interactions for which no images are available during training. In this section, we show that our method offers significant improvements over [9] for zero-shot HOI detection.

Table 2: mAPs (%) in the default setting for ZSD. This is the seen object setting, i.e., it assumes that all the objects have been seen.

Method	Unseen (120 classes)	Seen (480 classes)	All (600 classes)
Shen <i>et al.</i> [9]	5.62	-	6.26
Ours	<b>10.93</b>	12.60	<b>12.26</b>

Table 3: mAPs (%) in the unseen object setting for ZSD. This is the unseen object setting where the trained model for interaction recognition has not seen any examples of some object classes.

Method	Unseen (100 classes)	Seen (500 classes)	All (600 classes)
Ours	11.22	14.36	13.84

##### 4.4.1 Seen object scenario

We first consider the same setting as [9]. We select 120 relationship triplets ensuring that every object involved on these 120 relationships occurs in at least one of the remaining 480 triplets. We call this the “seen object” zero-shot setting, i.e., the model sees all the objects involved but not the exact relationships. Later, we will consider the “unseen object” setting as well where no relationships involving a particular set of objects will be observed during training.

Table 2 shows the performance of our approach in the “seen object” setting for 120 unseen triplets during training. We achieve significant improvement (5.3% absolute mAP) over the prior method for zero-shot interaction detection. Overall, on all 600 classes, our model gives 6% absolute improvement in mAP.

##### 4.4.2 Unseen object scenario

Now we introduce the “unseen object” setting for evaluating zero-shot HOI detection. We start by randomly selecting 12 objects from the 80 objects in HICO. We pick all the relationships containing these objects. This gives us 100 relationship triplets which constitute the test (unseen) set for zero-shot HOI detection. We train models using visual examples from only the remaining 500 categories. Table 3 gives results for our methods in this setting. We cannot compare with existing methods because none of them have the ability to detect HOIs in the unseen object scenario. We hope that our method will serve as a baseline for future research on this important problem.

In figure 4, we show that our model can detect interactions with objects for which no images are seen during training. This is because we use a generic detector which can detect many more objects. We note, here, that there are some classes among the 80 COCO classes which do not



Figure 4: Some HOI detections in the unseen object ZSD setting. Our model has not seen any image with the objects shown above during training. The first two rows are correct detections. While the last row shows some mistakes.

occur in OI. We willingly take the penalty for missing interactions involving these objects in order to present a more robust system which not only works for the dataset of interest but is able to generalize to completely unseen interaction classes (even the object was not seen). We believe that these are strong baselines for this setting and we will release class lists and training sets to standardize evaluation for future methods. We reiterate that none of the previous methods has the ability to detect HOIs in this scenario.

#### 4.5. Ablation Analysis

We point out that the generic object detector used for zero-shot HOI detection can also be used in the supervised setting. For example, using this detector, we obtain an mAP of 14.35% on the Full set of the HICO-Det dataset. This is a competitive performance and is better than most published work (table 1). This shows the strength of our generalization approach. In this section, we provide further analysis of our model with the generic object detector.

**Number of neighbours.** To demonstrate the effectiveness of generalization through our method, we vary the number of neighboring objects which are added to the dataset for each training instance. Table 4 shows the effect of using different number of neighbors. The baseline (first row) is when no additional objects are added. This is the case when we do not use any additional data and rely only on the interactions present in the original dataset. We successively add more neighboring objects to the training data and observe that the performance improves significantly. However, after about five additional neighbors, the performance starts to saturate because noise from clustering starts to make an

Table 4: HICO-Det performance (mAP %) of the model with different number of neighbors considered for the generalization module.

r (Number of objects)	Full (600 classes)	Rare (138 classes)	Non-rare (462 classes)
0	12.72	7.57	14.26
3	13.70	7.98	15.41
5	<b>14.35</b>	<b>9.84</b>	<b>15.69</b>
7	13.51	7.07	15.44

Table 5: mAPs (%) for different clustering methods.

Clustering Algorithm	Full (600 classes)	Rare (138 classes)	Non-rare (462 classes)
K means	<b>14.35</b>	<b>9.84</b>	15.69
Agglomerative	14.05	7.59	<b>15.98</b>
Affinity Propagation	13.49	7.53	15.28

impact. Because the clusters are not perfect, adding more neighbors can start becoming harmful. Also, the training times increase rapidly. Therefore, we add five neighbors for each HOI instance in all our experiments.

**Clustering method.** To check if another clustering algorithm might be better, we create clusters using different algorithms. From table 5 we observe that K-means clustering leads to the best performance. Hierarchical agglomerative clustering also gives close albeit lower performance.

**Importance of features.** Further ablation studies (table 6) showed that removing  $f_g$ , or  $f_h$  from the functional generalization module leads to a reduction in performance. For example, training the model without the geometric feature  $f_g$  gives an mAP of 12.43% and training the model without  $f_h$  in the generalization module gives an mAP of just 12.15%



Table 6: Ablation studies (mAP %).

Setting	Full (600 classes)	Rare (138 classes)	Non-rare (462 classes)
Base	<b>14.35</b>	<b>9.84</b>	<b>15.69</b>
Base $-f_h$	12.15	4.87	14.33
Base $-f_g$	12.43	8.02	13.75

showing the importance of both features in the model. In particular, note that the performance for rare classes in the absence of  $f_h$  is very low (4.87%). This shows that using visual information from the human is essential for detecting rare HOIs.

#### 4.6. Dealing with Dataset Bias

Dataset bias leads to models being biased towards particular classes [52]. In fact, bias in the training dataset is usually amplified by the models [19, 20]. Our proposed method can be used as a way to overcome the dataset bias problem. To illustrate this, we use metrics proposed in [19] to quantitatively study model bias.

We consider a set of (object, predicate) pairs  $\mathcal{Q} = \{(o_1, p_1), \dots, (o_2, p_2)\}$ . For each pair in  $\mathcal{Q}$ , we consider two scenarios: (1) the training set is heavily biased *against* the pair; (2) the training set is heavily biased *towards* the pair. For generating the training sets for a pair  $q_i = \{o_i, p_i\} \in \mathcal{Q}$ , for the first scenario, we remove all training samples containing the pair  $q_i$  and keep all other samples for the object. Similarly, for the second scenario, we remove all training samples containing  $o_i$  except those containing the pair  $q_i$ . For the pair,  $q_i$  the test set bias is  $b_i$  (We adopt the definition of bias from [19]. See supplementary materials for more details.). Given two models, the one with bias closer to test set bias is considered better. We show that our approach of augmenting the dataset brings the model bias closer to the test set bias. In particular, we consider  $\mathcal{Q} = \{(\text{horse}, \text{ride}), (\text{cup}, \text{hold})\}$ , such that  $b_1 = 0.275$  and  $b_2 = 0.305$ .

In the first scenario, baseline models trained on biased datasets have biases 0.124 and 0.184 for (horse, ride) and (cup, hold) respectively. Note that these are less than the test set biases because of the heavy bias against these pairs in their respective training sets. Next, we train models by augmenting the training sets using our methodology for only one neighbor of each object. Models trained on these new sets have biases 0.130 and 0.195. That is, our approach leads to a reduction in the bias *against* these pairs.

Similarly, for the second scenario, baseline models trained on the biased datasets have biases 0.498 and 0.513 for (horse, ride) and (cup, hold) respectively. Training models on datasets de-biased by our approach give biases 0.474 and 0.50. In this case, our approach leads to a reduction in the bias *towards* these pairs.

#### 4.7. Bonus Experiment: Visual Model

Our generalization module can be complementary to existing approaches. To illustrate this, we consider a simple visual module shown in figure 5. It takes the union of  $b_h$  and  $b_o$  and crops the union box from the image. It passes the cropped union box through a CNN. The feature obtained,  $f_u$  is concatenated with  $f_h$  and  $f_o$  and passed through two FC layers. This module and the generalization module independently predict the probabilities for predicates and the final prediction is the average of the two. Using the generic object detector, the combined model gives an mAP of 15.82% on the Full HICO-Det dataset. This is better than the published best of 14.84%. This experiment shows that the generalization methodology proposed in this paper is complementary to existing works which rely on purely visual data. Using our generalization module in conjugation with other existing methods can lead to performance improvements.

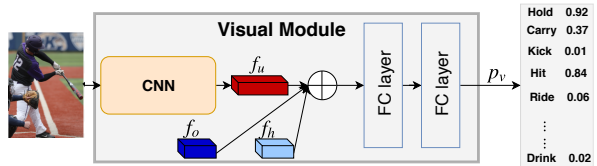


Figure 5: Simple visual module.

#### 5. Discussion

We discuss some limitations of the proposed approach. First, we assume that all predicates follow functional similarities. However, some predicates might only apply to particular objects. For example, you can `blow` a cake, but not a donut which is functionally similar to cake. Our current model does not capture such social constraints. Further work can focus on trying to explicitly incorporate such priors into the model. A related limitation of the proposed approach is the independence assumption on predicates. In fact, some predicates are completely dependent. For example, `straddle` usually implies `sit_on` for bicycles or horses. However, due to the in-exhaustive labeling of the datasets, we (and most previous work) ignore this dependence. Approaches exploiting co-occurrences of predicates can help overcome this problem.

#### 6. Conclusion

We have presented a way to enhance HOI detection by incorporating the common-sense idea that human-object interactions look similar for functionally similar objects. Our method is able to detect previously unseen (zero-shot) human-object relationships. We have provided experimental validation for our claims and have reported state-of-the-art results for the problem. However, there are still several



issues that need to be solved to advance the understanding of the problem and improve performance of models.

## Acknowledgement

This project was supported by the Intelligence Advanced Research Projects Activity (IARPA) via Department of Interior/Interior Business Center (DOI/IBC) contract number D17PC00345. The U.S. Government is authorized to reproduce and distribute reprints for Governmental purposes not withstanding any copyright annotation thereon.

**Disclaimer:** The views and conclusions contained herein are those of the authors and should not be interpreted as necessarily representing the official policies or endorsements, either expressed or implied of IARPA, DOI/IBC or the U.S. Government.

## References

- [1] Mohammad Amin Sadeghi and Ali Farhadi. Recognition using visual phrases. In *Computer Vision and Pattern Recognition (CVPR), 2011 IEEE Conference on*, pages 1745–1752. IEEE, 2011. 1
- [2] Saurabh Gupta and Jitendra Malik. Visual semantic role labeling. *arXiv preprint arXiv:1505.04474*, 2015. 1, 2
- [3] Yu-Wei Chao, Yunfan Liu, Xieyang Liu, Huayi Zeng, and Jia Deng. Learning to detect human-object interactions. *arXiv preprint arXiv:1702.05448*, 2017. 1, 2, 6
- [4] Georgia Gkioxari, Ross Girshick, Piotr Dollár, and Kaiming He. Detecting and recognizing human-object interactions. *arXiv preprint arXiv:1704.07333*, 2017. 1, 2, 6
- [5] Joseph Redmon, Santosh Divvala, Ross Girshick, and Ali Farhadi. You only look once: Unified, real-time object detection. In *CVPR*, pages 779–788. IEEE, 2016. 1
- [6] Ross Girshick. Fast r-cnn. In *ICCV*, pages 1440–1448. IEEE, 2015. 1
- [7] Shaoqing Ren, Kaiming He, Ross Girshick, and Jian Sun. Faster r-cnn: Towards real-time object detection with region proposal networks. In *NIPS*, pages 91–99, 2015. 1, 3, 12
- [8] Wei Liu, Dragomir Anguelov, Dumitru Erhan, Christian Szegedy, Scott Reed, Cheng-Yang Fu, and Alexander C Berg. Ssd: Single shot multibox detector. In *ECCV*, pages 21–37. Springer, 2016. 1
- [9] Liyue Shen, Serena Yeung, Judy Hoffman, Greg Mori, and Li Fei-Fei. Scaling human-object interaction recognition through zero-shot learning. In *2018 IEEE Winter Conference on Applications of Computer Vision (WACV)*, pages 1568–1576. IEEE, 2018. 1, 3, 6
- [10] Vincent Delaitre, Josef Sivic, and Ivan Laptev. Learning person-object interactions for action recognition in still images. In *Advances in neural information processing systems*, pages 1503–1511, 2011. 1, 2
- [11] Cewu Lu, Ranjay Krishna, Michael Bernstein, and Li Fei-Fei. Visual relationship detection with language priors. In *European Conference on Computer Vision*, pages 852–869. Springer, 2016. 1
- [12] Ranjay Krishna, Yuke Zhu, Oliver Groth, Justin Johnson, Kenji Hata, Joshua Kravitz, Stephanie Chen, Yannis Kalantidis, Li-Jia Li, David A Shamma, et al. Visual genome: Connecting language and vision using crowdsourced dense image annotations. *International Journal of Computer Vision*, 123(1):32–73, 2017. 1, 2
- [13] Bohan Zhuang, Qi Wu, Chunhua Shen, Ian Reid, and Anton van den Hengel. Care about you: towards large-scale human-centric visual relationship detection. *arXiv preprint arXiv:1705.09892*, 2017. 1, 2
- [14] Tomas Mikolov, Ilya Sutskever, Kai Chen, Gregory S. Corrado, and Jeffrey Dean. Distributed representations of words and phrases and their compositionality. In *NIPS*, 2013. 2, 3
- [15] JJ Gibson. The theory of affordances the ecological approach to visual perception (pp. 127-143), 1979. 2
- [16] Kaiming He, Xiangyu Zhang, Shaoqing Ren, and Jian Sun. Deep residual learning for image recognition. *2016 IEEE Conference on Computer Vision and Pattern Recognition (CVPR)*, pages 770–778, 2016. 2
- [17] Alina Kuznetsova, Hassan Rom, Neil Alldrin, Jasper Uijlings, Ivan Krasin, Jordi Pont-Tuset, Shahab Kamali, Stefan Popov, Matteo Mallocci, Tom Duerig, and Vittorio Ferrari. The open images dataset v4: Unified image classification, object detection, and visual relationship detection at scale. *arXiv:1811.00982*, 2018. 2, 3
- [18] Olga Russakovsky, Jia Deng, Hao Su, Jonathan Krause, Sanjeev Satheesh, Sean Ma, Zhiheng Huang, Andrej Karpathy, Aditya Khosla, Michael Bernstein, et al. Imagenet large scale visual recognition challenge. *International Journal of Computer Vision*, 115(3):211–252, 2015. 2
- [19] Jieyu Zhao, Tianlu Wang, Mark Yatskar, Vicente Ordonez, and Kai-Wei Chang. Men also like shopping: Reducing gender bias amplification using corpus-level constraints. *arXiv preprint arXiv:1707.09457*, 2017. 2, 8, 12
- [20] Lisa Anne Hendricks, Kaylee Burns, Kate Saenko, Trevor Darrell, and Anna Rohrbach. Women also snowboard: Overcoming bias in captioning models. In *Proceedings of the European Conference on Computer Vision (ECCV)*, pages 771–787, 2018. 2, 8, 12
- [21] Bangpeng Yao and Li Fei-Fei. Grouplet: A structured image representation for recognizing human and object interactions. In *Computer Vision and Pattern Recognition (CVPR), 2010 IEEE Conference on*, pages 9–16. IEEE, 2010. 2
- [22] Bangpeng Yao and Li Fei-Fei. Modeling mutual context of object and human pose in human-object interaction activities. In *Computer Vision and Pattern Recognition (CVPR), 2010 IEEE Conference on*, pages 17–24. IEEE, 2010. 2
- [23] Bangpeng Yao, Xiaoye Jiang, Aditya Khosla, Andy Lai Lin, Leonidas Guibas, and Li Fei-Fei. Human action recognition by learning bases of action attributes and parts. In *Computer Vision (ICCV), 2011 IEEE International Conference on*, pages 1331–1338. IEEE, 2011. 2

- [24] Abhinav Gupta and Larry S Davis. Objects in action: An approach for combining action understanding and object perception. In *Computer Vision and Pattern Recognition, 2007. CVPR'07. IEEE Conference on*, pages 1–8. IEEE, 2007. 2
- [25] Abhinav Gupta, Aniruddha Kembhavi, and Larry S Davis. Observing human-object interactions: Using spatial and functional compatibility for recognition. *IEEE Transactions on Pattern Analysis and Machine Intelligence*, 31(10):1775–1789, 2009. 2
- [26] Chaitanya Desai and Deva Ramanan. Detecting actions, poses, and objects with relational phraselets. In *European Conference on Computer Vision*, pages 158–172. Springer, 2012. 2
- [27] Yu-Wei Chao, Zhan Wang, Yugeng He, Jiaxuan Wang, and Jia Deng. Hico: A benchmark for recognizing human-object interactions in images. In *Proceedings of the IEEE International Conference on Computer Vision*, pages 1017–1025, 2015. 2, 5
- [28] Bingjie Xu, Junnan Li, Yongkang Wong, Mohan S Kankanhalli, and Qi Zhao. Interact as you intend: Intention-driven human-object interaction detection. *arXiv preprint arXiv:1808.09796*, 2018. 3, 6
- [29] Alexander Kolesnikov, Christoph H Lampert, and Vittorio Ferrari. Detecting visual relationships using box attention. *arXiv preprint arXiv:1807.02136*, 2018. 3
- [30] Siyuan Qi, Wenguan Wang, Baoxiong Jia, Jianbing Shen, and Song-Chun Zhu. Learning human-object interactions by graph parsing neural networks. *arXiv preprint arXiv:1808.07962*, 2018. 3, 6
- [31] Keizo Kato, Yin Li, and Abhinav Gupta. Compositional learning for human object interaction. In *Proceedings of the European Conference on Computer Vision (ECCV)*, pages 234–251, 2018. 3
- [32] Arun Mallya and Svetlana Lazebnik. Learning models for actions and person-object interactions with transfer to question answering. In *European Conference on Computer Vision*, pages 414–428. Springer, 2016. 3
- [33] Rohit Girdhar and Deva Ramanan. Attentional pooling for action recognition. In *Advances in Neural Information Processing Systems*, pages 34–45, 2017. 3
- [34] Hao-Shu Fang, Jinkun Cao, Yu-Wing Tai, and Cewu Lu. Pairwise body-part attention for recognizing human-object interactions. *arXiv preprint arXiv:1807.10889*, 2018. 3
- [35] Yongqin Xian, Bernt Schiele, and Zeynep Akata. Zero-shot learning-the good, the bad and the ugly. *arXiv preprint arXiv:1703.04394*, 2017. 3, 6
- [36] Soravit Changpinyo, Wei-Lun Chao, Boqing Gong, and Fei Sha. Synthesized classifiers for zero-shot learning. In *Proceedings of the IEEE Conference on Computer Vision and Pattern Recognition*, pages 5327–5336, 2016. 3
- [37] Elyor Kodirov, Tao Xiang, and Shaogang Gong. Semantic autoencoder for zero-shot learning. *arXiv preprint arXiv:1704.08345*, 2017. 3
- [38] Christoph H Lampert, Hannes Nickisch, and Stefan Harmeling. Attribute-based classification for zero-shot visual object categorization. *IEEE Transactions on Pattern Analysis and Machine Intelligence*, 36(3):453–465, 2014. 3
- [39] Ankan Bansal, Karan Sikka, Gaurav Sharma, Rama Chellappa, and Ajay Divakaran. Zero-shot object detection. In *The European Conference on Computer Vision (ECCV)*, September 2018. 3, 6
- [40] Berkan Demirel, Ramazan Gokberk Cinbis, and Nazli Ikizler-Cinbis. Zero-shot object detection by hybrid region embedding. *arXiv preprint arXiv:1805.06157*, 2018. 3
- [41] Shafin Rahman, Salman Khan, and Fatih Porikli. Zero-shot object detection: Learning to simultaneously recognize and localize novel concepts. *arXiv preprint arXiv:1803.06049*, 2018. 3
- [42] Jonathan Huang, Vivek Rathod, Chen Sun, Menglong Zhu, Anoop Korattikara, Alireza Fathi, Ian Fischer, Zbigniew Wojna, Yang Song, Sergio Guadarrama, et al. Speed/accuracy trade-offs for modern convolutional object detectors. In *IEEE CVPR*, volume 4, 2017. 3
- [43] Bohan Zhuang, Lingqiao Liu, Chunhua Shen, and Ian Reid. Towards context-aware interaction recognition. *arXiv preprint arXiv:1703.06246*, 2017. 4
- [44] George A Miller. Wordnet: a lexical database for english. *Communications of the ACM*, 38(11):39–41, 1995. 4
- [45] Mark Everingham, Luc Van Gool, Christopher KI Williams, John Winn, and Andrew Zisserman. The pascal visual object classes (voc) challenge. *International journal of computer vision*, 88(2):303–338, 2010. 5
- [46] Tsung-Yi Lin, Michael Maire, Serge Belongie, James Hays, Pietro Perona, Deva Ramanan, Piotr Dollár, and C Lawrence Zitnick. Microsoft coco: Common objects in context. In *European conference on computer vision*, pages 740–755. Springer, 2014. 5
- [47] Chen Gao, Yuliang Zou, and Jia-Bin Huang. ican: Instance-centric attention network for human-object interaction detection. *arXiv preprint arXiv:1808.10437*, 2018. 5, 6, 12
- [48] Julia Peyre, Ivan Laptev, Cordelia Schmid, and Josef Sivic. Weakly-supervised learning of visual relations. In *ICCV 2017-International Conference on Computer Vision 2017*, 2017. 5
- [49] Tanmay Gupta, Alexander Schwing, and Derek Hoiem. No-frills human-object interaction detection: Factorization, appearance and layout encodings, and training techniques. *arXiv preprint arXiv:1811.05967*, 2018. 6, 12
- [50] Yong-Lu Li, Siyuan Zhou, Xijie Huang, Liang Xu, Ze Ma, Hao-Shu Fang, Yan-Feng Wang, and Cewu Lu. Transferable interactiveness prior for human-object interaction detection. *arXiv preprint arXiv:1811.08264*, 2018. 6, 12
- [51] Julia Peyre, Ivan Laptev, Cordelia Schmid, and Josef Sivic. Detecting rare visual relations using analogies. *arXiv preprint arXiv:1812.05736*, 2018. 6, 12
- [52] Antonio Torralba and Alexei A Efros. Unbiased look at dataset bias. 2011. 8

- [53] T. Lin, P. Dollar, R. Girshick, K. He, B. Hariharan, and S. Belongie. Feature pyramid networks for object detection. In *2017 IEEE Conference on Computer Vision and Pattern Recognition (CVPR)*, pages 936–944, Los Alamitos, CA, USA, jul 2017. IEEE Computer Society. 12



## S. Supplementary Material

### S.1. Assumptions about number of parameters

To study the efficiency of each method, we compute the number of parameters introduced by the corresponding method. Some works [49] have all the details, necessary for the computation, in their manuscript, while some [47, 50, 51] fail to mention the specifics. Hence, we made the following assumptions while estimating the number of parameters. Note that only those methods, where sufficient details weren't mentioned in the paper, are discussed. Since all of the methods use an object detector in the first step, we compute the number of parameters introduced by the detector. Table S1 shows the number of parameters estimated for each method.

Table S1: Estimated parameters(in millions) for the detectors used in a few of the state-of-the-art methods.

Method	Detector	Backbone Architecture	# Params (in millions)
ICAN [47]	FPN [53]	ResNet-50	40.9
Gupta <i>et al.</i> [49]	Faster-RCNN [7]	ResNet-152	63.7
Interactiveness Prior [50]	Faster-RCNN [7]	ResNet-50	29
Peyre <i>et al.</i> [51]	FPN [53]	ResNet-50	40.9
Ours	Faster-RCNN [7]	ResNet-101	48

#### S.1.1 ICAN

Authors in [47] use two fully connected layers in each of the human, object, and pairwise streams, but the details of the hidden layers were not mentioned in their work. The feature dimensions of the human and object stream are 3072, while for the pairwise stream it is 5408. To make a conservative estimate, we assume the dimensions of the hidden layers to be 1024 and 512 for the human and object stream. For the pairwise stream we assume dimensions of 2048 and 512 for the hidden layers. We end up with an estimated total of 48.1M parameters for their architecture. This gives the total parameters for their method to be **89M** (48.1+ 40.9 (Detector; see table S1)).

#### S.1.2 Interactiveness Prior

Li *et al.* [50] used a FasterRCNN [7] based detector with a ResNet-50 backbone architecture. In their proposed approach, they have 10 MLPs (multi-layer perceptrons) with two layers each and 3 fully connected (FC) layers. Out of the 10 MLPs, we estimated, 6 of them to have an input dimension of 2048, 3 of them to have 1024 and one of them 3072. The dimension of hidden layers was given to be 1024 for all the 10 MLPs. The 3 FC layers have input dimensions of 1024 and an output dimension 117. This makes the number of parameters utilized equal to 35M. Their total number of parameters = **64M** (35 + 29 (detector)).

#### S.1.3 Peyre *et al.*

Peyre *et al.* used a FPN [53] detector with a ResNet-50 backbone. They have a total of 9 MLPs with two hidden layers each, and 3 FC layers. The input dimension of the FC layers is 2048 and the output dimension is 300. 6 of the 9 MLPs have an input dimension of 300 and an output dimension of 1024. Another 2 of the 9 MLPs have input dimension of 1000 and 900 respectively. Their output dimension is 1024. We assume the dimensions of the hidden layers in all these MLPs to be 1024 and 1024. The last of the 9 MLPs has an input dimension of 8 and an output dimension of 400. We assume a hidden layer of dimension 256 for this MLP. This brings the estimated parameter used to 21.8M and their total parameter count = **62.7M** (21.8 + 40.9 (detector)).

### S.2. Bias details

Adopting the bias metric from [19], we define the bias for a verb-object pair,  $(v_*, o)$  in a set as:

$$b_s(v_*, o) = \frac{c_s(v_*, o)}{\sum_v c_s(v, o)} \quad (2)$$

where,  $c_s(v, o)$  is the number of instances of the pair  $(v, o)$  in the set,  $s$ . This measure can be used to quantify the bias for a verb-object pair in a dataset or for a model's prediction. For a dataset,  $\mathcal{D}$ ,  $c_{\mathcal{D}}(v, o)$  gives the number of instances of  $(v, o)$  pairs in it. Therefore,  $b_{\mathcal{D}}$  represents the bias for the pair  $(v_*, o)$  in the dataset. A low value ( $\approx 0$ ) of  $b_{\mathcal{D}}$  means that the set is heavily biased against the pair while a high value ( $\approx 1$ ) means that it is heavily biased towards the pair.

Similarly, we can define the bias of a model by considering the model's predictions as the dataset under consideration. For example, suppose that the model under consideration gives the predictions  $\mathcal{P}$  for the dataset  $\mathcal{D}$ . We can define the model's bias as:

$$b_{\mathcal{P}}(v_*, o) = \frac{c_{\mathcal{P}}(v_*, o)}{\sum_v c_{\mathcal{P}}(v, o)} \quad (3)$$

where,  $c_{\mathcal{P}}(v, o)$  gives the number of instances of the pair  $(v, o)$  in the set of the model's predictions  $\mathcal{P}$ .

A perfect model is one whose bias,  $b_{\mathcal{P}}(v_*, o)$  is equal to the dataset bias  $b_{\mathcal{D}}(v_*, o)$ . However, due to bias amplification [19, 20], most models will have a higher/lower bias than the test dataset depending on the training set bias. That is, if the training set is heavily biased towards (resp. against) a pair, then the model's predictions will be more heavily biased towards (resp. against) that pair for the test set. The aim of a bias reduction method should be to bring the model's bias closer to the test set bias. Our experiments in the paper showed that our proposed algorithm is able to reduce the gap between the test set bias and the model prediction bias.